Theoretical Chemistry Accounts (2020) 139:30
https://doi.org/10.1007/s00214-019-2539-6

REGULAR ARTICLE

Scaling exchange and correlation in the on-top density functional of multiconfiguration pair-density functional theory: effect on electronic excitation energies and bond energies

Davide Presti[1,3] · Jan Kadlec[1,2,4] · Donald G. Truhlar[1] · Laura Gagliardi[1]

Received: 25 September 2019 / Accepted: 19 December 2019 / Published online: 23 January 2020

Abstract
Multiconfiguration pair-density functional (MC-PDFT) theory provides an economical way to calculate the ground-state and excited-state energetics of strongly correlated systems. The energy is calculated from the kinetic energy, density, and on-top pair-density of a multiconfiguration wave function as the sum of kinetic energy, classical Coulomb energy, and on-top density functional energy. We have usually found good results with the translated Perdew–Burke–Ernzerhof (tPBE) on-top density functional, and in this article, we examine whether the results can be systematically improved by introducing scaling constants into the exchange and correlation terms. We find that only a small improvement is possible for electronic excitation energies and that no improvement is possible for bond energies.

Keywords Excitation energies · Bond energies · Benchmark · MC-PDFT · Pair-density · On-top pair-density functionals

1 Introduction

Electronically excited states play a key role in many branches of chemistry, including photochemistry [1], photosynthesis [2], and optoelectronic material function [3–6]. Modeling electronically excited states remains a major challenge for modern electronic structure theories because they are usually strongly correlated due to near degeneracy effects. Kohn–Sham density functional theory (KS-DFT) is widely used for ground-state properties, and time-dependent Kohn–Sham density functional theory (TD-KS-DFT) is widely used to determine excitation energies. This approach works more satisfactorily for valence excited states than for charge transfer and Rydberg excitations [7–12]. Moreover, even modern functionals do not always provide satisfactory performance in describing multiconfigurational systems.

Multiconfiguration pair-density functional theory (MC-PDFT) [13, 14] is an alternative to KS-DFT for excited states and multiconfigurational systems in general, and it has been shown to give promising results for atomic [13], organic [15–20], and inorganic systems [21], including transition metal species [22, 23] and heavy atoms [24, 25]. Unlike complete active space second-order perturbation theory (CASPT2) [26, 27] and multireference configuration interaction (MRCI), the cost of an MC-PDFT calculation is dominated by the cost of the parent multiconfigurational self-consistent field (MCSCF) calculation. MC-PDFT usually provides results comparable in accuracy to those of CASPT2, and therefore it is an appealing alternative to

"Festschrift in honor of Prof. Fernando R. Ornellas" guest Edited by Adélia Justino Aguiar Aquino, Antonio Gustavo Sampaio de Oliveira Filho & Francisco Bolivar Correto Machado.

Electronic supplementary material The online version of this article (https://doi.org/10.1007/s00214-019-2539-6) contains supplementary material, which is available to authorized users.

✉ Donald G. Truhlar
truhlar@umn.edu

✉ Laura Gagliardi
gagliard@umn.edu

[1] Department of Chemistry, Chemical Theory Center, and Minnesota Supercomputing Institute, University of Minnesota, Minneapolis 55455-0431, USA

[2] Institute of Organic Chemistry and Biochemistry, Czech Academy of Sciences, Flemingovo nám. 2, 16610 Prague 6, Czech Republic

[3] Present Address: Dipartimento di Chimica Industriale, Università degli Studi di Bologna, Viale del Risorgimento 4, 40136 Bologna, Italy

[4] Present Address: Department of Neurobiology, Weizmann Institute of Science, 76100 Rehovot, Israel

CASPT2 because of the significantly reduced computational costs, in terms of both memory and time requirements.

In MC-PDFT, the energy is computed from the kinetic energy and the classical Coulomb energy of an MCSCF wave function (third and fourth terms of Eq. 1) and from an on-top density functional (last term of Eq. 1) depending on the total electronic density $\rho(\boldsymbol{r})$, its gradient, and the on-top pair-density $\Pi(\boldsymbol{r})$ [28, 29], where $\mathbf{r}$ denotes a point in space

$$E^{MC-PDFT} = V_{NN} + V_{Ne}(\rho(\boldsymbol{r})) + \langle \Psi^{MCSCF}|T|\Psi^{MCSCF}\rangle + V_{C}(\rho(\boldsymbol{r})) + E_{ot}[\rho(\boldsymbol{r}), |\nabla\rho|, \Pi(\boldsymbol{r})] \quad (1)$$

where V_{NN} and $V_{Ne}(\rho(\boldsymbol{r}))$ denote the nuclear repulsion and the electron–nucleus attraction, respectively.

The currently used on-top density functionals are translations of existing KS-DFT functionals. The most widely studied functional is the translated PBE (tPBE [13, 14]) functional, which has a translated exchange term and a translated correlation term (see Ref. [13] for details on "translation" of density functionals). In this study, we explore the effect of multiplying the exchange term by a constant S_X and multiplying the correlation term by a constant S_C. The tPBE functional with this scaling will be abbreviated tPBE (S_X, S_C), where the standard tPBE energy corresponds to $E^{MC-PDFT}$ = tPBE (1.0, 1.0). The functional scaling is motivated by recent work in the context of KS-DFT, where it was shown that using $S_X = 1.25$ and $S_C = 0.5$ [30, 31] for PBE (this scaling being labeled "HLE": high local exchange) provides an improved description of molecular electronic excitations, including those of Rydberg type, and of semiconductor band gaps. A main advantage of KS-DFT local functionals (such as PBE and HLE-type functionals) is the absence of static correlation error caused by the presence of HF exchange [32–34]. On the other hand, the MCSCF wave function in MC-PDFT includes nonlocal MCSCF exchange; thus, only local on-top functionals are used (in their translated form), although these functionals have not been optimized for MC-PDFT. However, given the similarities between local KS-DFT functionals and local translated on-top functionals, the study of functional scaling in MC-PDFT helps to understand how electronic properties are affected by changes in the functional. For example, it was observed that increasing the exchange contribution improves the valence singlet and triplet $\pi\pi^*$ excitation energies for benzene at the MC-PDFT level [20]. Calculations with these special values of S_X and S_C were previously labeled HLE in the context of KS-DFT, and so, we also use that label in the context of MC-PDFT, i.e., tPBE (1.25, 0.5) ≡ tPBE–HLE.

We considered wide ranges of values for S_X and S_C, and we report the mean signed and unsigned errors (MSEs and MUEs) with respect to the experimental or accurate theoretical data available in the literature. For electronic excitations (Tables 1 and 2), we report the results obtained with tPBE (1.1, 0.5), which we found to be perform best of all examined scalings, although no significant improvement on average is obtained with respect to tPBE. Note that, as compared to previous work, we updated many of the reference values to which we compare with the FCI/CBS estimates from the recent work of Loos et al. [35] that are reported for some of the electronic excitations. (The retained old reference values and the new ones are reported in Table S4 of ESM.) We also count the number of cases with an error below 0.28 eV—which was chosen (somewhat arbitrarily) as the borderline between reasonably successful and unsuccessful.

Table 1 Spin-forbidden atomic excitation energies (eV). The reference values are taken from the experimental data

		AS[a]	CASSCF	CASPT2	tPBE	tPBE–HLE	tPBE (1.1,0.5)	References
Be	$^1S \rightarrow {}^3P$	(2,4)	2.86	2.78	2.55	2.48	2.47	2.73 [55]
C	$^3P \rightarrow {}^1D$	(4,4)	1.56	1.27	1.06	1.59	1.33	1.26 [56]
N^+	$^3P \rightarrow {}^1D$	(4,4)	2.19	1.91	1.51	2.18	1.85	1.89 [56]
N	$^4S \rightarrow {}^2D$	(5,4)	2.79	2.51	2.05	2.99	2.53	2.38 [56]
O^+	$^4S \rightarrow {}^2D$	(5,4)	3.78	3.44	2.78	3.94	3.36	3.32 [57]
O	$^3P \rightarrow {}^1D$	(6,4)	2.23	1.99	1.27	1.83	1.55	1.96 [56]
Sc^+	$^3D \rightarrow {}^1D$	(2,6)	0.37	0.32	0.47	0.55	0.53	0.30 [58]
Mn	$^6S \rightarrow {}^8P$	(7,9)	2.19	2.38	2.15	1.76	1.92	2.15 [58]
Co	$^4F \rightarrow {}^2F$	(9,6)	2.29	0.40	0.89	− 0.01[b]	0.71	0.89 [58]
Mo	$^7S \rightarrow {}^5S$	(6,6)	1.66	1.67	2.00	2.52	2.28	1.34 [59]
Ru	$^5F \rightarrow {}^3F$	(8,6)	0.97	0.95	1.08	1.37	1.23	0.78 [60]
	MUE[c]		0.35	0.15	0.31	0.50	0.27	

[a]Active space (see pages S2–S3 of ESM to see how active spaces are defined). The numbers (*m, n*) indicate *m* active electrons in *n* active orbitals

[b]The tPBE–HLE functional gives the wrong sign

[c]Mean unsigned error

Table 2 Spin-conserving molecular excitation energies (eV) of the EE27/19 database)

		N^a	AS[b]	CASSCF	CASPT2	tPBE	tPBE–HLE	tPBE (1.1,0.5)	References
n→*π* valence*									
Acetaldehyde	$^1A''$	2	(12,12)	4.56	4.27	4.28	4.21	4.22	**4.31** [35][c]
Acetone	$^1A_2$	2	(12,12)	4.71	4.44	4.47	4.38	4.40	4.43 [61]
Formaldehyde	$^1A_2$	2	(12,10)	4.73	3.89	3.89	3.85	3.86	**3.97** [35]
Pyrazine	$^1B_{3u}$	3	(10,10)	5.08	4.04	3.96	4.16	4.06	3.97 [62, 63]
Pyridazine	$^1B_1$	2	(10,10)	4.63	3.67	3.50	3.71	3.60	3.60 [61]
Pyridine	$^1B_1$	3	(8,8)	5.64	5.06	5.06	4.95	5.00	4.74 [64, 65]
Pyrimidine	$^1B_1$	2	(10,10)	4.97	4.39	4.34	4.40	4.36	4.18 [66]
s-tetrazine	$^1B_{3u}$	2	(14,14)	3.65	2.56	2.54	2.82	2.68	2.25 [61]
π→*π* valence*									
N_2	$^1\Sigma_u^-$	1	(6,6)	10.90	9.88	9.58	9.91	9.73	**9.91** [35]
Ethylene	$^1B_{1u}$	5	(4,10)	7.72	8.16	6.93	8.12	7.19	**7.91** [35]
Butadiene	^1B_u	4	(10,15)	6.38	6.51	6.18	6.58	6.22	6.21 [67]
Cyclopentadiene	$^1B_2$	1	(4,4)	7.35	5.51	4.12	4.68	4.37	5.26 [68, 69]
Benzene	$^1B_{2u}$	2	(6,13)	4.99	4.83	5.04	4.72	4.88	4.90 [70]
”	$^3B_{1u}$	1	(6,13)	3.94	3.99	4.28	3.91	4.09	4.12 [71]
Naphthalene	$^1B_{3u}$	2	(10,10)	4.24	4.21	4.38	4.07	4.23	4.00 [72]
”	$^3B_{2u}$	1	(10,10)	3.04	3.18	3.32	3.05	3.18	3.11 [71]
Furan	$^1B_2$	2	(6,10)	6.69	6.32	6.47	6.26	6.33	6.06 [73]
”	$^3B_2$	1	(6,10)	3.93	4.07	4.21	3.78	3.99	4.17 [71]
Hexatriene	^1B_u	2	(6,12)	5.78	5.31	5.46	5.25	5.34	4.93 [74]
	^3B_u	1	(6,12)	2.88	2.66	2.74	2.64	2.69	2.69 [71]
Other valence									
Be	^1P	1	(2,4)	6.19	5.71	4.36	5.20	4.75	5.28 [55]
N_2	$^1\Pi_g$	1	(6,6)	11.87	9.40	8.64	9.13	8.86	**9.33** [35]
Rydberg									
Water	$^1B_1$	2	(8,9)	7.69	7.61	7.45	8.44	7.62	**7.70** [35]
”	$^3B_1$	1	(8,9)	7.16	7.19	7.09	7.86	7.18	**7.33** [35]
π→*π* charge transfer*									
*p*NA[d]	$^1A_1$	3	(12,12)	6.09	4.64	3.95	3.89	3.94	4.30[e]
DMABN[f]	$^1A_1$	3	(12,12)	6.18	4.87	4.28	4.44	4.36	4.57 [75]
B-TCNE[g]	$^1A_1$	2	(4,4)	4.48	3.84	3.63	3.48	3.58	3.59 [76]
Valence MUE				0.72	0.17	0.32	0.20	0.24	
Rydberg MUE				0.09	0.12	0.24	0.64	0.11	
Charge transfer MUE				1.43	0.30	0.22	0.22	0.19	
Total MUE				**0.75**	**0.18**	**0.30**	**0.24**	**0.22**	

[a]*N* is the number of states whose energies are averaged in the CASSCF and is also the number of states in the model space in MS-CASPT2 calculations

[b]The numbers (*m, n*) indicate *m* active electrons in *n* active orbitals (see pages S2–S3 of ESM to see how active spaces are defined)

[c]Theoretical FCI/CBS estimates from Loos et al. (see Table 6 of Ref. [35]) are highlighted in bold

[d]Intramolecular charge transfer in *p*NA

[e]*δ*–CR-EOMCC(2,3), D, see Refs. [77, 78]

[f]DMABN is a case with intramolecular charge transfer

[g]There is intermolecular charge transfer in the B-TCNE complex

Although the present work is concerned only with MC-PDFT, we note that some previous work [36–38] employed range-separated on-top density functionals in other kinds of hybrid multiconfigurational theories.

2 Databases

We consider three databases: SFAEE11, EE27/19, and DBE6.

SFAEE11 contains eleven spin-changing excitations of atomic systems (investigated previously with MC-PDFT in Ref. [13]), including both light atoms and transition metals. We do not include spin–orbit coupling in any of the calculations. For atomic excitation energies, we removed spin–orbit coupling from the experimental values by considering for each state the weighted average of the multiplet's energy.

EE27 includes the 27 spin-conserving excitation energies: the 23 in the previously defined EE23 database [16, 39] containing valence, Rydberg, and intramolecular and intermolecular charge transfer transitions of organic molecules plus the Be valence $s \rightarrow p$ excitation, the N_2 valence $\sigma \rightarrow \pi^*$ and $\pi \rightarrow \pi^*$ excitations, and the cyclopentadiene $^1B_2$ valence $\pi \rightarrow \pi^*$ excitation. We updated the database from the values used previously by using the more accurate data of Loos et al. [35] where available. The updated database is called EE27/19, and full details of the update are given in electronic supplementary material (ESM).

DBE6 contains six bond energies (investigated previously with MC-PDFT in Ref. [13]) that are examples of strongly correlated systems.

The values we report for MUE in the article are based on deviations from the reference data. Electronic supplementary material contains MSEs.

3 Methods

3.1 General

We report results for CASSCF, CASPT2, and MC-PDFT. All MC-PDFT [13] calculations employed the tPBE, tPBE–HLE, or tPBE (S_x, S_c) on-top density functionals. All calculations are gas-phase calculations performed using *Molcas 8.2* [40].

CASSCF [41] calculations employed a level shift of 1.0 E_h (1 $E_h \equiv 1$ hartree = 27.211 eV). The Cholesky decomposition [42] algorithm is used throughout with a threshold of 10^{-8} E_h. The numbers of active electrons and active orbitals in each active space (AS) are given in the tables of the main text, and further details are given in Table S1. (Tables and figures with the prefix S are in ESM.)

CASPT2 calculations were performed for comparison, using an imaginary shift of 0.2 E_h and the default value (0.25 E_h [43]) for the IPEA shift. The state average (SA) method [44] was applied to organic molecules' excitations as indicated in Table 2 of the manuscript considering N states. For these systems, the multistate (MS) method [45] was used for CASPT2 [26, 27] calculations.

The keywords "Atom" and "Linear" were employed to impose spherical and linear symmetry in the case of atoms and linear molecules, respectively. The highest spatial symmetry operator (D_{2h}) was employed for the excitation energies of Be, N, N_2, O^+, Co, Mn, and Ru (see Table 1). For all the organic molecules and diatomic molecules reported in Tables 2 and 3, no spatial symmetry was imposed, except for cyclopentadiene and NiCl. (The C_{2v} symmetry operator was applied in both of those cases.)

For Cr_2, NiCl, and the transition metal atoms, the second-order Douglas–Kroll–Hess Hamiltonian [46, 47] was used; all the other calculations are nonrelativistic.

For calculating bond energies, in every case the geometry is optimized with the method under consideration. (Sometimes, this is called using "consistently optimized geometries.")

3.2 Basis sets

The cc-pVTZ basis set [48] was used for main group atoms, for CaO, and for the singlet-to-singlet Be excitation energy. The aug-cc-pVTZ basis set [49] was used for the excitation energies of N_2.

Table 3 Bond energies (in eV)

	AS[a]	CASSCF	CASPT2	tPBE	tPBE–HLE	References
H_2	(2,2)	4.13	4.59	4.68	4.74	4.75 [79]
N_2	(6,6)	8.84	9.39	9.78	9.36	9.74 [80]
F_2	(2,2)	0.71	1.49	2.12	2.14	1.66 [81]
Cr_2	(12,12)	0.00[b]	0.99[c]	0.59	− 1.78[d]	1.47 [82]
CaO	(8,8)	3.99	3.59	4.44	5.99	4.22 [83]
NiCl	(11,12)	2.71	3.94	4.10	5.67	3.97 [84, 85]
	MUE	**0.91**	**0.30**	**0.30**	**1.27**	

[a]Active space (please refer to pages S2–S3 of ESM to see how active spaces are defined)

[b]The CASSCF dissociation curve of Cr_2 (Figure S7 of ESM) does not have a minimum at R_e (Ref. 1.68 Å [82])

[c]The CASPT2 minimum energy is erroneously located at 2.65 Å

[d]The tPBE–HLE functional gives the wrong sign

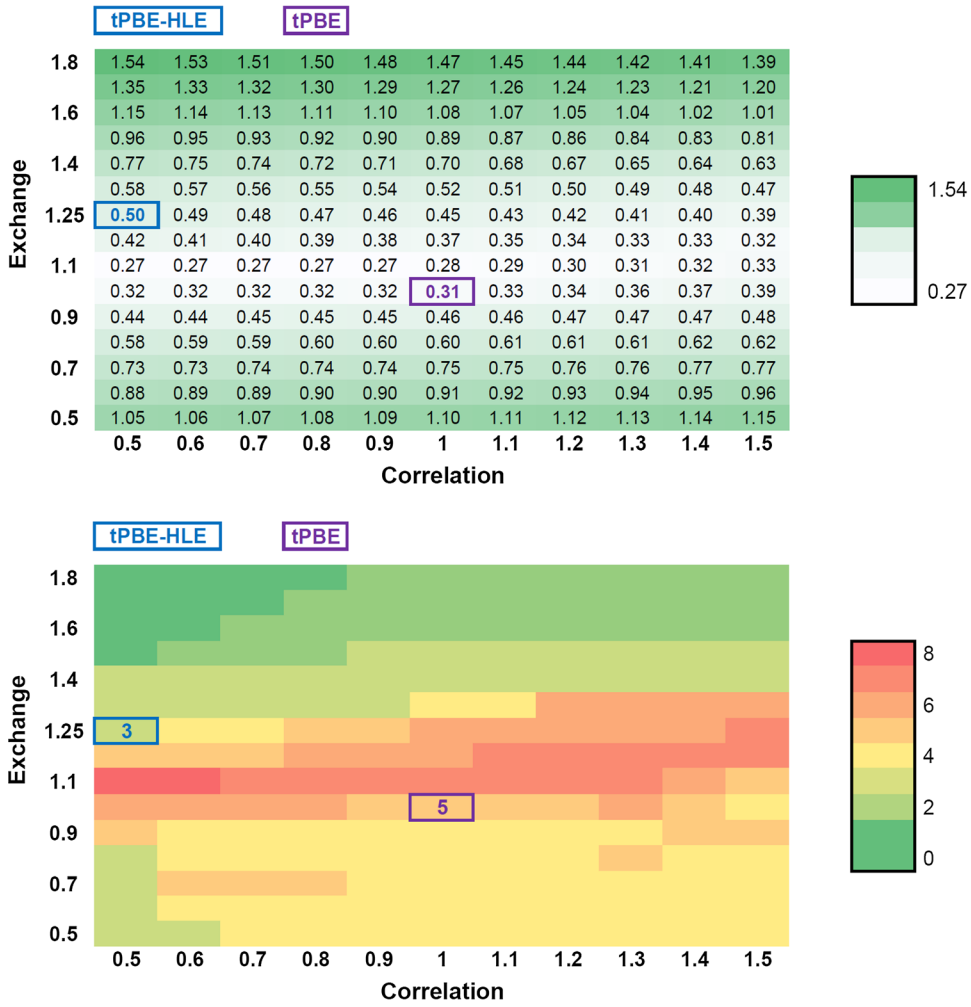

Fig. 1 (Top) Mean unsigned error (MUE in eV) for the SFAEE11 database (see Table 1) with respect to the amount of exchange and correlation for the tPBE functional. The tPBE and tPBE–HLE MUEs are highlighted. (Bottom) Number of systems that have, for each combination of exchange and correlation, a maximum absolute deviation (from the benchmark) less than or equal to 0.28 eV, out of a total of 11 spin-forbidden atomic excitations. The tPBE and tPBE–HLE results are highlighted with numerical values

The cc-pVTZ-DK basis set [50] was used for Cr_2. The ANO-RCC-VTZP basis set [51] was used for NiCl and transition metals in SFAEE11.

The jul-cc-pVTZ basis set [52] was used for molecules in EE27/19 with valence excitations, except for cyclopentadiene, for which the cc-pVTZ basis set was used. The aug-cc-pVTZ basis set was employed for water, the 6-31 + G** basis set [53, 54] was employed for *para*-nitroaniline (*p*NA) and 4-(dimethylamino)-benzonitrile (DMABN), and the aug-cc-pVTZ basis set was used for the benzene–tetracyanoethylene (B-TCNE) complex.

4 Results and discussion for excitation energies

The results for the SFAEE11 database of spin-forbidden atomic excitation energies are reported in Table 1. The table shows that CASSCF overestimates the atomic excitation energies by an average of 0.35 eV. CASPT2 provides the smallest errors with respect to the reference data, with an MUE of 0.15 eV. The tPBE functional performs fairly well for atomic excitations (MUE of 0.31 eV), though still giving larger errors than CASPT2. The tPBE–HLE functional gives a larger MUE (0.50 eV) than tPBE and in general overestimates the excitation energies; the error is especially large for Mo and Ru atoms, whereas the Co $^4F \rightarrow {}^2F$ excitation is underestimated by tPBE–HLE by 0.9 eV, resulting in an erroneous negative sign.

Figure 1 shows that errors can be reduced if the exchange is scaled by 1.1 and correlation by any factor in the range 0.5–0.9. Figure 1 also shows that one obtains the most accurate predictions with $S_X = 1.1$ and $S_C = 0.5$–0.6, but this does not markedly improve the results obtained with the unscaled tPBE pair-density functional (MUE of 0.27 eV for tPBE (1.1, 0.5) vs. 0.31 eV for tPBE). It is perhaps significant though that the tPBE (1.1, 0.5) functional, which is much more similar to tPBE–HLE than to tPBE, gives a reasonable Co $^4F \rightarrow {}^2F$ excitation energy.

The results for the EE27/19 database of spin-conserving excitations energies are reported in Table 2. The EE27/19 database contains 22 valence excitations, two Rydberg

transitions, and three charge transfer transitions. CASSCF gives the largest deviations with respect to the reference data, especially for valence excitations (MUE 0.72 eV) and charge transfer excitations (MUE 1.43 eV). CASPT2 give better results, although charge transfer excitations are still overestimated (MUE 0.30 eV).

The cyclopentadiene valence $\pi \rightarrow \pi^*$ excitation, which is well predicted by CASPT2 (5.51 eV) with respect to experiment (5.26 eV), remains problematic for both tPBE and tPBE–HLE (underestimated by more than 0.5 eV). Overall, tPBE–HLE is better than tPBE for valence excitations, but less accurate for Rydberg excitations. The top panel of Fig. 2 shows that again one gets the best results with tPBE (1.1, 0.5), with the MUE being reduced from 0.30 to 0.22 eV. The bottom panel of Fig. 2 shows the number of systems, out of 27, that have an absolute deviation lower than or equal to 0.28 eV; this value is the largest for $S_X = 1.1$–1.2 and $S_C = 0.5$–0.7 (for tPBE (1.1, 0.5) there are 20 systems with this accuracy), whereas it corresponds to 15 and 18 systems for tPBE and tPBE–HLE, respectively. However, the improvement given by tPBE (1.1, 0.5) over tPBE and tPBE–HLE is modest and involves mostly the two Rydberg excitations.

5 Results and discussion for bond energies

Table 3 presents the results for six bond energies. These include the Cr_2 molecule, whose ground-state dissociation is particularly difficult to describe. The tPBE–HLE bond energy has the wrong sign, and its MUE is therefore increased to 1.27 eV, higher even than for CASSCF (MUE 0.90 eV). Figure 3 shows that the original tPBE exchange–correlation scaling provides the most reliable results for bond energies. It also shows, somewhat amazingly, that no improvement can be gained on average by scaling exchange and/or correlation. The original tPBE functional slightly outperforms CASPT2 for both energy values and the qualitatively correct behavior of dissociation curves, which are shown in ESM.

Bond energies appear to be very sensitive to parameter scaling, especially the exchange term. In contrast to

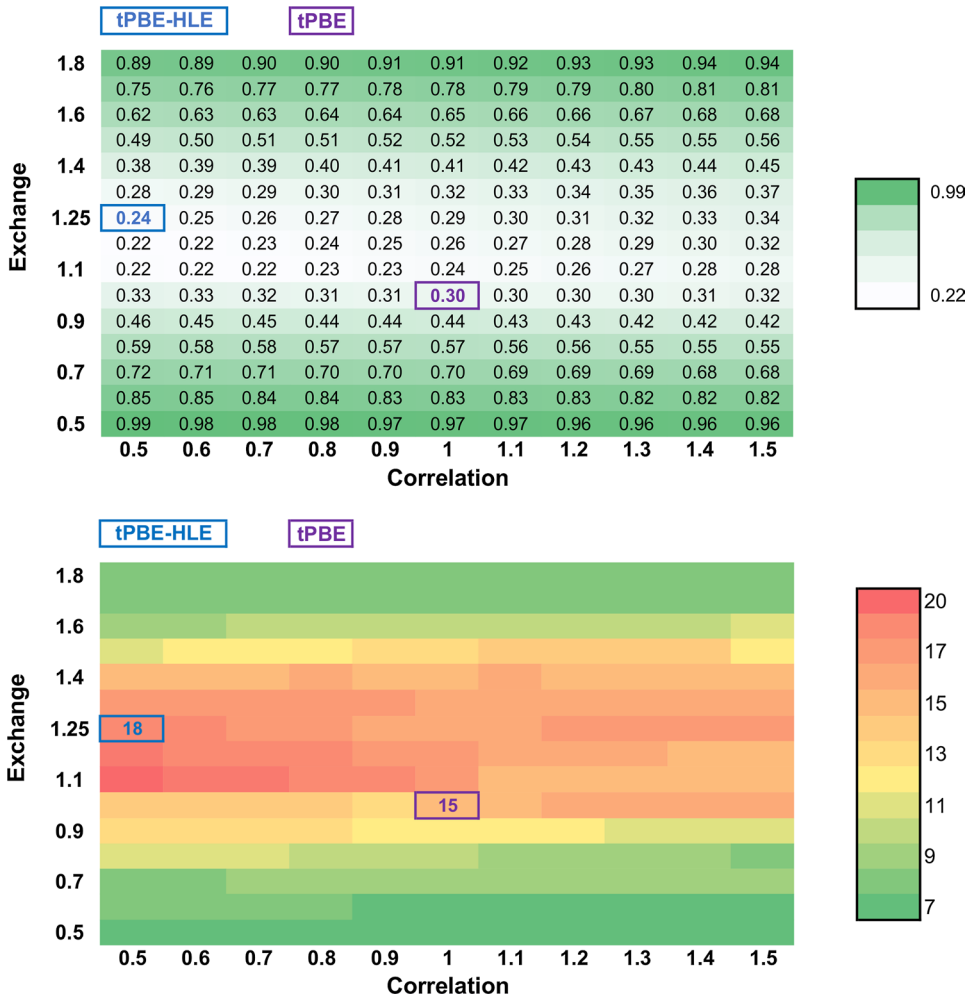

Fig. 2 Results for EE27/19 database statistics of spin-conserving atomic excitation energies. (Top) MUEs (in eV) reported for each combination of exchange and correlation. (Bottom) Heat map showing the number of systems (out of 27) with maximum absolute deviation less than or equal to 0.28 eV. The tPBE and tPBE–HLE values are highlighted

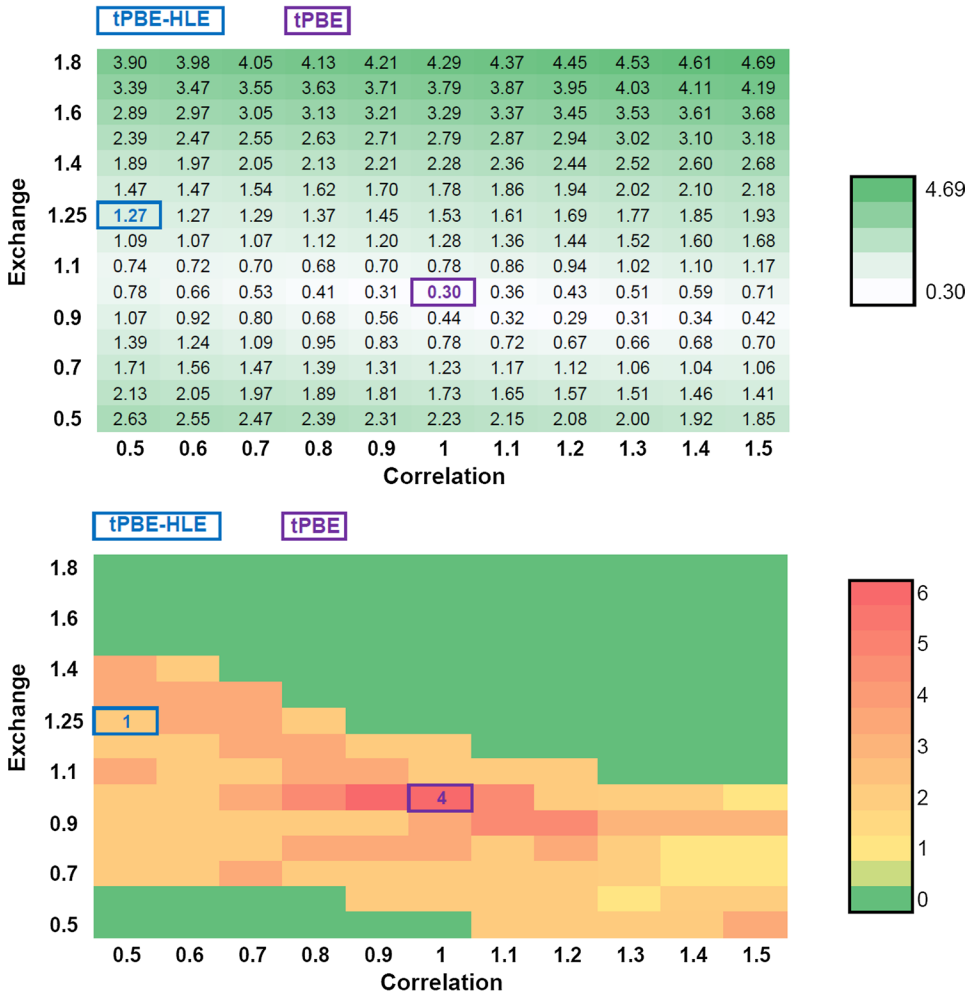

Fig. 3 (Top) Mean unsigned error (MUE) in eV for six bond energies (see Table 3) with respect to the amount of exchange and correlation for the tPBE functional. The tPBE and tPBE–HLE MUEs are highlighted. (Bottom) Number of systems that have, for each combination of exchange and correlation, a maximum absolute deviation (from the benchmark) less than or equal to 0.28 eV, out of a total of six bond energies (see Table 3). The tPBE and tPBE–HLE results are highlighted with numerical values

excitation energies, which are discussed above, the best combination is given by $S_X = 1.0$ and $S_C = 0.9$–1.1, yet this suffices to suitably describe only 4 systems out of 6. This suggests that a simple functional scaling is not sufficient to obtain on-top density functionals that perform broadly and significantly better than the ones we have been using.

6 Conclusions

We investigated how the scaling of exchange and correlation contributions of on-top density functionals in MC-PDFT affects properties such as atomic and molecular excitation energies and bond dissociation energies. A new combination of excitation energies for spin-conserving excitation energies including valence, Rydberg and CT excitation was introduced as database EE27/19 for this study, and we also compared to spin-forbidden atomic excitation energies and to bond energies.

The results are that only a small improvement in excitation energies over those obtained with the original tPBE functional can be obtained by scaling the exchange and correlation components of the tPBE on-top density functional (with $S_X = 1.1$ and $S_C = 0.5$), and no improvement at all can be obtained for the mean unsigned error in bond energies. We thus conclude that the development of significantly improved on-top density functionals will require either new or more flexible functional forms rather than just scaling parameters.

7 Electronic supplementary information

Further information about the computational details, basis sets, active spaces and dissociation curves; Cartesian coordinates for the EE27/19 database. (PDF) CASSCF orbital files in Molcas format (.RasOrb) in compressed archive (RAR).

Acknowledgements This work was supported by the National Science Foundation under grant CHE–1746186.

Compliance with ethical standards

Conflict of interest The authors declare that they have no conflict of interest.

References

1. Olivucci M, Sinicropi A (2005) Computational photochemistry. In: Theoretical and computational chemistry series, vol 16. Elsevier, pp 1–33
2. Cheng Y-C, Fleming GR (2009) Dynamics of light harvesting in photosynthesis. Annu Rev Phys Chem 60:241–262. https://doi.org/10.1146/annurev.physchem.040808.090259
3. Johnston MB, Herz LM (2016) Hybrid perovskites for photovoltaics: charge-carrier recombination, diffusion, and radiative efficiencies. Acc Chem Res 49:146–154. https://doi.org/10.1021/acs.accounts.5b00411
4. Presti D, Pedone A, Ciofini I et al (2016) Optical properties of the dibenzothiazolylphenol molecular crystals through ONIOM calculations: the effect of the electrostatic embedding scheme. Theor Chem Acc. https://doi.org/10.1007/s00214-016-1808-x
5. Presti D, Labat F, Pedone A et al (2016) Modeling emission features of salicylidene aniline molecular crystals: a QM/QM' approach. J Comput Chem 37:861–870. https://doi.org/10.1002/jcc.24282
6. Presti D, Wilbraham L, Targa C et al (2017) Understanding aggregation-induced emission in molecular crystals: insights from theory. J Phys Chem C 121:5747–5752. https://doi.org/10.1021/acs.jpcc.7b00488
7. Dreuw A, Head-Gordon M (2004) Failure of time-dependent density functional theory for long-range charge-transfer excited states: the Zincbacteriochlorin–Bacteriochlorin and Bacteriochlorophyll–Spheroidene Complexes. J Am Chem Soc 126:4007–4016. https://doi.org/10.1021/ja039556n
8. Li R, Zheng J, Truhlar DG (2010) Density functional approximations for charge transfer excitations with intermediate spatial overlap. Phys Chem Chem Phys 12:12697–12701. https://doi.org/10.1039/C0CP00549E
9. Zhao Y, Truhlar DG (2006) Density functional for spectroscopy: no long-range self-interaction error, good performance for Rydberg and charge-transfer states, and better performance on average than B3LYP for ground states. J Phys Chem A 110:13126–13130. https://doi.org/10.1021/jp066479k
10. Tawada Y, Tsuneda T, Yanagisawa S et al (2004) A long-range-corrected time-dependent density functional theory. J Chem Phys 120:8425–8433. https://doi.org/10.1063/1.1688752
11. Yanai T, Tew DP, Handy NC (2004) A new hybrid exchange–correlation functional using the Coulomb-attenuating method (CAM-B3LYP). Chem Phys Lett 393:51–57. https://doi.org/10.1016/j.cplett.2004.06.011
12. Vydrov OA, Wu Q, Van Voorhis T (2008) Self-consistent implementation of a nonlocal van der Waals density functional with a Gaussian basis set. J Chem Phys 129:014106. https://doi.org/10.1063/1.2948400
13. Li Manni G, Carlson RK, Luo S et al (2014) Multiconfiguration pair-density functional theory. J Chem Theory Comput 10:3669–3680. https://doi.org/10.1021/ct500483t
14. Gagliardi L, Truhlar DG, Li Manni G et al (2017) Multiconfiguration pair-density functional theory: a new way to treat strongly correlated systems. Acc Chem Res 50:66–73. https://doi.org/10.1021/acs.accounts.6b00471
15. Ghosh S, Sonnenberger AL, Hoyer CE et al (2015) Multiconfiguration pair-density functional theory outperforms Kohn–Sham density functional theory and multireference perturbation theory for ground-state and excited-state charge transfer. J Chem Theory Comput 11:3643–3649. https://doi.org/10.1021/acs.jctc.5b00456
16. Hoyer CE, Ghosh S, Truhlar DG, Gagliardi L (2016) Multiconfiguration pair-density functional theory is as accurate as CASPT2 for electronic excitation. J Phys Chem Lett 7:586–591. https://doi.org/10.1021/acs.jpclett.5b02773
17. Carlson RK, Truhlar DG, Gagliardi L (2015) Multiconfiguration pair-density functional theory: a fully translated gradient approximation and its performance for transition metal dimers and the spectroscopy of Re2Cl82–. J Chem Theory Comput 11:4077–4085. https://doi.org/10.1021/acs.jctc.5b00609
18. Presti D, Truhlar DG, Gagliardi L (2018) Intramolecular charge transfer and local excitation in organic fluorescent photoredox catalysts explained by RASCI-PDFT. J Phys Chem C 122:12061–12070. https://doi.org/10.1021/acs.jpcc.8b01844
19. Dong SS, Gagliardi L, Truhlar DG (2018) Excitation spectra of retinal by multiconfiguration pair-density functional theory. Phys Chem Chem Phys 20:7265–7276. https://doi.org/10.1039/c7cp07275a
20. Sharma P, Bernales V, Knecht S et al (2019) Density matrix renormalization group pair-density functional theory (DMRG-PDFT): singlet-triplet gaps in polyacenes and polyacetylenes. Chem Sci 10:1716–1723. https://doi.org/10.1039/c8sc03569e
21. Sharma P, Truhlar DG, Gagliardi L (2018) Multiconfiguration pair-density functional theory investigation of the electronic spectrum of MnO4-. J Chem Phys 148:124305. https://doi.org/10.1063/1.5021185
22. Stoneburner SJ, Gagliardi L (2018) air separation by catechol-ligated transition metals: a quantum chemical screening. J Phys Chem C 122:22345–22351. https://doi.org/10.1021/acs.jpcc.8b03599
23. Presti D, Stoneburner SJ, Truhlar DG, Gagliardi L (2019) Full correlation in a multiconfigurational study of bimetallic clusters: restricted active space pair-density functional Theory study of [2Fe-2S] systems. J Phys Chem C 123:11899–11907. https://doi.org/10.1021/acs.jpcc.9b00222
24. Gaggioli CA, Gagliardi L (2018) Theoretical investigation of plutonium-based single-molecule magnets. Inorg Chem 57:8098–8105. https://doi.org/10.1021/acs.inorgchem.8b00170
25. Ramirez BL, Sharma P, Eisenhart RJ et al (2019) Bimetallic nickel–lutetium complexes: tuning the properties and catalytic hydrogenation activity of the Ni site by varying the Lu coordination environment. Chem Sci 10:3375–3384. https://doi.org/10.1039/C8SC04712J
26. Andersson K, Malmqvist PA, Roos BO et al (1990) Second-order perturbation theory with a CASSCF reference function. J Phys Chem 94:5483–5488
27. Andersson K, Malmqvist P, Roos BO (1992) Second-order perturbation theory with a complete active space self-consistent field reference function. J Chem Phys 96:1218–1226. https://doi.org/10.1063/1.462209
28. Becke AD, Savin A, Stoll H (1995) Extension of the local-spin-density exchange-correlation approximation to multiplet states. Theor Chim Acta 91:147–156. https://doi.org/10.1007/BF01114982
29. Staroverov VN, Davidson ER (2000) Charge densities for singlet and triplet electron pairs. Int J Quantum Chem 77:651–660. https://doi.org/10.1002/(SICI)1097-461X(2000)77:3%3c651:AID-QUA6%3e3.0.CO;2-N
30. Verma P, Truhlar DG (2017) HLE16: a local Kohn–Sham gradient approximation with good performance for semiconductor band gaps and molecular excitation energies. J Phys Chem Lett 8:380–387. https://doi.org/10.1021/acs.jpclett.6b02757

31. Verma P, Truhlar DG (2017) HLE17: an improved local exchange-correlation functional for computing semiconductor band gaps and molecular excitation energies. J Phys Chem C 121:7144–7154. https://doi.org/10.1021/acs.jpcc.7b01066
32. Miehlich B, Stoll H, Savin A (1997) A correlation-energy density functional for multideterminantal wavefunctions. Mol Phys 91:527–536. https://doi.org/10.1080/002689797171418
33. Gräfenstein J, Cremer D (2005) Development of a CAS-DFT method covering non-dynamical and dynamical electron correlation in a balanced way. Mol Phys 103:279–308
34. Yu HS, Li SL, Truhlar DG (2016) Perspective: Kohn–Sham density functional theory descending a staircase. J Chem Phys. https://doi.org/10.1063/1.4963168
35. Loos PF, Scemama A, Blondel A et al (2018) A mountaineering strategy to excited states: highly accurate reference energies and benchmarks. J Chem Theory Comput 14:4360–4379. https://doi.org/10.1021/acs.jctc.8b00406
36. Sharkas K, Savin A, Jensen HJA, Toulouse J (2012) A multiconfigurational hybrid density-functional theory. J Chem Phys 137:864. https://doi.org/10.1063/1.4733672
37. Garza AJ, Bulik IW, Henderson TM, Scuseria GE (2015) Synergy between pair coupled cluster doubles and pair density functional theory. J Chem Phys. https://doi.org/10.1063/1.4906607
38. Garza AJ, Bulik IW, Henderson TM, Scuseria GE (2015) Range separated hybrids of pair coupled cluster doubles and density functionals. Phys Chem Chem Phys 17:22412–22422. https://doi.org/10.1039/c5cp02773j
39. Isegawa M, Truhlar DG (2013) Valence excitation energies of alkenes, carbonyl compounds, and azabenzenes by time-dependent density functional theory: linear response of the ground state compared to collinear and noncollinear spin-flip TDDFT with the Tamm–Dancoff approximation. J Chem Phys 138:134111. https://doi.org/10.1063/1.4798402
40. Aquilante F, Autschbach J, Carlson RK et al (2016) Molcas 8: new capabilities for multiconfigurational quantum chemical calculations across the periodic table. J Comput Chem 37:506–541. https://doi.org/10.1002/jcc.24221
41. Roos BO, Taylor PR, Siegbahn PEM (1980) A complete active space SCF method (CASSCF) using a density matrix formulated super-CI approach. Chem Phys 48:157–173. https://doi.org/10.1016/0301-0104(80)80045-0
42. Aquilante F, Lindh R, Bondo Pedersen T (2007) Unbiased auxiliary basis sets for accurate two-electron integral approximations. J Chem Phys 127:114107. https://doi.org/10.1063/1.2777146
43. Ghigo G, Roos BO, Malmqvist P-Å (2004) A modified definition of the zeroth-order Hamiltonian in multiconfigurational perturbation theory (CASPT2). Chem Phys Lett 396:142–149. https://doi.org/10.1016/j.cplett.2004.08.032
44. Stålring J, Bernhardssonn A, Lindh R (2001) Analytical gradients of a state average MCSCF state and a state average diagnostic. Mol Phys 99:103–114. https://doi.org/10.1080/00268970011000 5642
45. Finley J, Malmqvist P-Å, Roos BO, Serrano-Andrés L (1998) The multi-state CASPT2 method. Chem Phys Lett 288:299–306. https://doi.org/10.1016/S0009-2614(98)00252-8
46. Douglas M, Kroll NM (1974) Quantum electrodynamical corrections to the fine structure of helium. Ann Phys (N Y) 82:89–155. https://doi.org/10.1016/0003-4916(74)90333-9
47. Wolf A, Reiher M, Hess BA (2002) The generalized Douglas–Kroll transformation. J Chem Phys 117:9215–9226. https://doi.org/10.1063/1.1515314
48. Dunning TH (1989) Gaussian basis sets for use in correlated molecular calculations. I. The atoms boron through neon and hydrogen. J Chem Phys 90:1007–1023. https://doi.org/10.1063/1.456153
49. Kendall RA, Dunning TH, Harrison RJ (1992) Electron affinities of the first-row atoms revisited. Systematic basis sets and wave functions. J Chem Phys 96:6796–6806. https://doi.org/10.1063/1.462569
50. Balabanov NB, Peterson KA (2005) Systematically convergent basis sets for transition metals. I. All-electron correlation consistent basis sets for the 3d elements Sc-Zn. J Chem Phys 123:064107. https://doi.org/10.1063/1.1998907
51. Roos BO, Lindh R, Malmqvist P-Å et al (2004) Main group atoms and dimers studied with a new relativistic ANO basis set. J Phys Chem A 108:2851–2858. https://doi.org/10.1021/jp031064+
52. Papajak E, Truhlar DG (2011) Convergent partially augmented basis sets for post-Hartree–Fock calculations of molecular properties and reaction barrier heights. J Chem Theory Comput 7:10–18. https://doi.org/10.1021/ct1005533
53. Hehre WJ, Ditchfield R, Pople JA (1972) Self-consistent molecular orbital methods. XII. Further extensions of Gaussian—type basis sets for use in molecular orbital studies of organic molecules. J Chem Phys 56:2257–2261. https://doi.org/10.1063/1.1677527
54. Francl MM, Pietro WJ, Hehre WJ et al (1982) Self-consistent molecular orbital methods. XXIII. A polarization-type basis set for second-row elements. J Chem Phys 77:3654–3665. https://doi.org/10.1063/1.444267
55. Kramida A, Martin WC (1997) A compilation of energy levels and wavelengths for the spectrum of neutral beryllium (Be l). J Phys Chem Ref Data 26:1185–1194. https://doi.org/10.1063/1.555999
56. Moore CE (1993) CRC series in evaluated data in atomic physics. CRC Press, Boca Raton
57. Martin WC, Kaufman V, Musgrove A (1993) A compilation of energy levels and wavelengths for the spectrum of singly-ionized oxygen (O II). J Phys Chem Ref Data 22:1179–1212. https://doi.org/10.1063/1.555928
58. Sugar J, Corliss C (1985) Atomic energy levels of the iron-period elements: potassium through nickel. J Phys Chem Ref Data 14(Suppl 2):1–664
59. Sugar J, Musgrove A (1988) Energy levels of molybdenum, Mo I through Mo XLII. J Phys Chem Ref Data 17:155–239. https://doi.org/10.1063/1.555818
60. Moore CE (1971) Reference Data Series 35. National Bureau of Standards, Washington, DC
61. Caricato M, Trucks GW, Frisch MJ, Wiberg KB (2010) Electronic transition energies: a study of the performance of a large range of single reference density functional and wave function methods on valence and Rydberg states compared to experiment. J Chem Theory Comput 6:370–383. https://doi.org/10.1021/ct9005129
62. Walker IC, Palmer MH (1991) The electronic states of the azines. IV. Pyrazine, studied by VUV absorption, near-threshold electron energy-loss spectroscopy and ab initio multi-reference configuration interaction calculations. Chem Phys 153:169–187. https://doi.org/10.1016/0301-0104(91)90017-N
63. Weber P, Reimers JR (1999) Ab initio and density functional calculations of the energies of the singlet and triplet valence excited states of pyrazine. J Phys Chem A 103:9821–9829. https://doi.org/10.1021/jp991403s
64. Walker IC, Palmer MH, Hopkirk A (1990) The electronic states of the azines. II. Pyridine, studied by VUV absorption, near-threshold electron energy loss spectroscopy and ab initio multi-reference configuration interaction calculations. Chem Phys 141:365–378. https://doi.org/10.1016/0301-0104(90)87070-R
65. Cai ZL, Reimers JR (2000) The Low-lying excited states of pyridine. J Phys Chem A 104:8389–8408. https://doi.org/10.1021/jp000962s
66. Ferreira da Silva F, Almeida D, Martins G et al (2010) The electronic states of pyrimidine studied by VUV photoabsorption and electron energy-loss spectroscopy. Phys Chem Chem Phys 12:6717–6731. https://doi.org/10.1039/b927412j

67. Watson MA, Chan GKL (2012) Excited states of butadiene to chemical accuracy: reconciling theory and experiment. J Chem Theory Comput 8:4013–4018. https://doi.org/10.1021/ct300591z
68. Bolovinos A, Tsekeris P, Philis J et al (1984) Absolute vacuum ultraviolet absorption spectra of some gaseous azabenzenes. J Mol Spectrosc 103:240–256. https://doi.org/10.1016/0022-2852(84)90051-1
69. Frueholz RP, Flicker WM, Mosher OA, Kuppermann A (1979) Electronic spectroscopy of 1,3-cyclopentadiene, 1,3-cyclohexadiene and 1,3-cycloheptadiene by electron impact. J Chem Phys 70:2003–2013. https://doi.org/10.1063/1.437626
70. Hiraya A, Shobatake K (1991) Direct absorption spectra of jet-cooled benzene in 130–260 nm. J Chem Phys 94:7700–7706. https://doi.org/10.1063/1.460155
71. Schreiber M, Silva-Junior MR, Sauer SPA, Thiel W (2008) Benchmarks for electronically excited states: CASPT2, CC2, CCSD, and CC3. J Chem Phys 128:134110. https://doi.org/10.1063/1.2889385
72. Huebner RH, Meilczarek SR, Kuyatt CE (1972) Electron energy-loss spectroscopy of naphthalene vapor. Chem Phys Lett 16:464–469. https://doi.org/10.1016/0009-2614(72)80401-9
73. Flicker WM, Mosher OA, Kuppermann A (1976) Electron impact investigation of electronic excitations in furan, thiophene, and pyrrole. J Chem Phys 64:1315–1321. https://doi.org/10.1063/1.432397
74. Leopold DG, Pendley RD, Roebber JL et al (1984) Direct absorption spectroscopy of jet-cooled polyenes. II. The 11Bu+←11Ag- transitions of butadienes and hexatrienes. J Chem Phys 81:4218–4229. https://doi.org/10.1063/1.447453
75. Druzhinin SI, Mayer P, Stalke D et al (2010) Intramolecular charge transfer with 1-tert-butyl-6-cyano-1,2,3,4-tetrahydroquinoline (NTC6) and other aminobenzonitriles. A comparison of experimental vapor phase spectra and crystal structures with calculations. J Am Chem Soc 132:7730–7744. https://doi.org/10.1021/ja101336n
76. Stein T, Kronik L, Baer R (2009) Reliable prediction of charge transfer excitations in molecular complexes using time-dependent density functional theory. J Am Chem Soc 131:2818–2820. https://doi.org/10.1021/ja8087482
77. Piecuch P, Kucharski SA, Kowalski K, Musiał M (2002) Efficient computer implementation of the renormalized coupled-cluster methods: the R-CCSD[T], R-CCSD(T), CR-CCSD[T], and CR-CCSD(T) approaches. Comput Phys Commun 149:71–96. https://doi.org/10.1016/S0010-4655(02)00598-2
78. Kowalski K, Piecuch P (2004) New coupled-cluster methods with singles, doubles, and noniterative triples for high accuracy calculations of excited electronic states. J Chem Phys 120:1715–1738. https://doi.org/10.1063/1.1632474
79. Huber KP, Herzberg G, Huber KP, Herzberg G (1979) Constants of diatomic molecules. Van Nostrand Reinhold, New York
80. Lofthus A, Krupenie PH (1977) The spectrum of molecular nitrogen. J Phys Chem Ref Data 6:113–307. https://doi.org/10.1063/1.555546
81. Bytautas L, Ruedenberg K (2005) Correlation energy extrapolation by intrinsic scaling. IV. Accurate binding energies of the homonuclear diatomic molecules carbon, nitrogen, oxygen, and fluorine. J Chem Phys 122:154110. https://doi.org/10.1063/1.1869493
82. Casey SM, Leopold DG (1993) Negative ion photoelectron spectroscopy of chromium dimer. J Phys Chem 97:816–830. https://doi.org/10.1021/j100106a005
83. Vasiliu M, Feller D, Gole JL, Dixon DA (2010) Structures and heats of formation of simple alkaline earth metal compounds: fluorides, chlorides, oxides, and hydroxides for Be, Mg, and Ca. J Phys Chem A 114:9349–9358. https://doi.org/10.1021/jp1050657
84. Jiang W, Deyonker NJ, Determan JJ, Wilson AK (2012) Toward accurate theoretical thermochemistry of first row transition metal complexes. J Phys Chem A 116:870–885. https://doi.org/10.1021/jp205710e
85. Zhang W, Truhlar DG, Tang M (2013) Tests of exchange-correlation functional approximations against reliable experimental data for average bond energies of 3d transition metal compounds. J Chem Theory Comput 9:3965–3977. https://doi.org/10.1021/ct400418u